

Lithological mapping in the Central Eastern Desert of Egypt using ASTER data

Reda Amer*, Timothy Kusky, Abduwasit Ghulam

Department of Earth and Atmospheric Sciences and Center for Environmental Sciences, Saint Louis University, St. Louis, MO 63103, USA

ARTICLE INFO

Article history:

Received 9 October 2008
Received in revised form 21 May 2009
Accepted 9 June 2009
Available online 14 June 2009

Keywords:

Lithological mapping
Remote sensing
ASTER image processing
Central Eastern Desert of Egypt

ABSTRACT

This study presents new methods for using Advanced Spaceborne Thermal Emission and Reflection Radiometer (ASTER) data for lithological mapping in arid environments. Visible, near-infrared and short wave infrared reflectance data have been processed and interpreted for mapping ophiolitic and granitic rocks at Fawakhir, Central Eastern Desert of Egypt. Image spectra show that the ophiolitic lithological members (serpentinites, metagabbros, and metabasalts), grey granite, and pink granite have absorption features around spectral bands 3, 6, and 8. ASTER band ratios $((2 + 4)/3, (5 + 7)/6, (7 + 9)/8)$ in RGB are constructed by summing the bands representing the shoulders of absorption features as a numerator, and the band located nearest the absorption feature as a denominator to discriminate between different ophiolitic and granitic rocks. The results show that ASTER band ratios $((2 + 4)/3, (5 + 7)/6, (7 + 9)/8)$ in a Red–Green–Blue (RGB) color combination identifies the ophiolitic rocks (serpentinites, metagabbros, and metabasalts) much better than previously published ASTER band ratios analysis. A Principal Component Analysis (PCA) was also implemented to reduce redundant information in highly correlated bands. PCA (5, 4, 2) in RGB enabled the discrimination between ophiolitic rocks and between the grey granite and pink granite. Thus, this technique is also recommended for mapping different types of granitic rocks. A new up-to-date lithologic map of the Fawakhir area is proposed based on the interpretation of ASTER image results and field verification work. It is concluded that the proposed methods have great potential for lithological mapping in arid and semi arid regions with similar climate and rock units as the Central Eastern Desert of Egypt.

© 2009 Elsevier Ltd. All rights reserved.

1. Introduction

The igneous and metamorphic terranes of Africa and Arabia on both sides of the Red Sea are parts of the Arabian Nubian Shield. The Arabian Nubian Shield was formed by suturing of smaller terranes consisting of arcs, accretionary prisms, and back arc basins that formed in the Mozambique Ocean (Stern, 1994), and were then brought together during the collision between East and West Gondwana to form what is known the East African orogen, about 600 Ma ago (Stern, 1994; Kusky et al., 2003). The Central Eastern Desert is almost exclusively built up of ophiolitic mélange and associated rocks, accreted arcs, together with subordinate molasse-type sediments and late-tectonic volcanics and granitoid intrusives (El Ramly et al., 1993). The Fawakhir area is located 93 km west of the Red Sea coast, along the Qift–Quseir highway in the Eastern Desert of Egypt at Lat. $26^{\circ}00'17''N$, and Long. $33^{\circ}35'42''E$. The Fawakhir area is occupied mainly by ophiolitic mélange represented by serpentinites, metagabbro, and metabasalt, then intruded by granitic rocks, and overlain by Hammamat sediments (Fig. 1).

Orbital remote sensing technology has progressed to advanced levels that are useful for lithological mapping as well as identifying mineral deposits (Abrams et al., 1983; Abrams and Hook, 1995; Sabins, 1997; Rowan and Mars, 2003; Rowan et al., 2003; Mars and Rowan, 2006; Gad and Kusky, 2007). Landsat Thematic Mapper (TM) Red–Green–Blue (RGB) band ratios $(5/7, 5/1, 5/4 * 3/4)$ have been used for mapping serpentinites in the Eastern Desert of Egypt (Sultan et al., 1986). They concluded that these band ratios can be used to distinguish serpentinites from the surrounding mafic rocks with high amounts of magnetite and hydroxyl-bearing minerals in arid regions. Gad and Kusky (2006) used Landsat Enhanced Thematic Mapper Plus (ETM*) band ratios $(5/3, 5/1, 7/5)$ and $(7/5, 5/4, 3/1)$ for mapping serpentinites in Barramiya area in the Central Eastern Desert of Egypt. They suggested that these band ratios can be used as well as the Sultan et al. (1986) band ratios for mapping serpentinites in the Eastern Desert of Egypt. An Advanced Spaceborne Thermal Emission and Reflection Radiometer (ASTER) band ratios image $(4/7, 4/6, 4/10)$ was used by Gad and Kusky (2006) for mapping the granite and metamorphic belt of the Wadi Kid area of Sinai, Egypt. They concluded that these band ratios can be used for mapping metamorphic rocks in the Arabian Nubian Shield and other arid regions. Abdeen et al. (2001) used ASTER RGB band ratios $(4/7, 4/1, 2/3 * 4/3)$ and $(4/7, 3/4, 2/1)$ for mapping ophiolites,

* Corresponding author. Tel.: +1 314 425 9648; fax: +1 314 977 3117.
E-mail address: ramer@slu.edu (R. Amer).

metasediments, volcanics, and granitoid lithologic units of the Neoproterozoic Allaqi Suture in southern Eastern Desert of Egypt.

The published ASTER band ratios of Abdeen et al. (2001) cannot better identify the contact between serpentinite and adjacent ophiolitic metagabbro and metabasalts, nor can they be used to

differentiate grey granite from pink granite. This study aims to develop new methods for using ASTER data in lithological mapping in arid and semiarid regions using Principal Component Analysis (PCA) and different combinations of band ratios, and to update the lithologic map of the Fawakhir area.

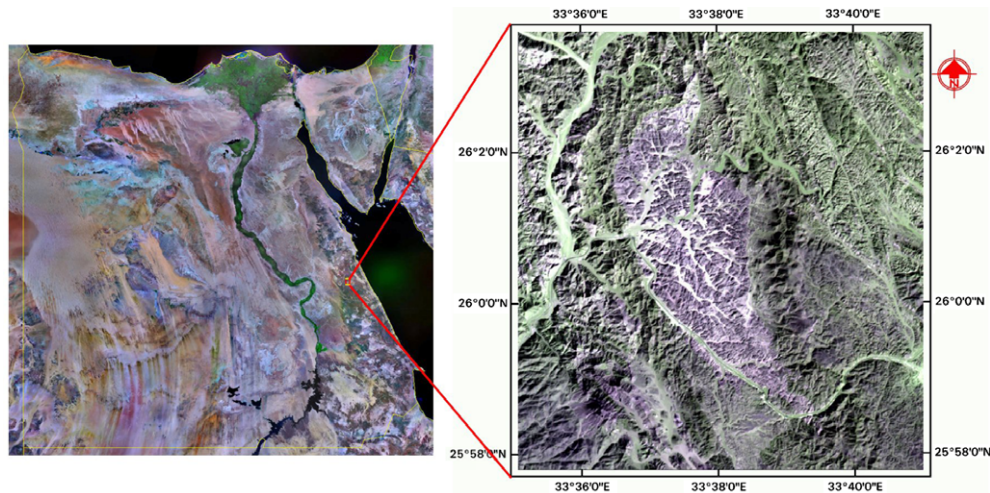


Fig. 1. Location map of the Fawakhir area on a satellite image of Egypt. (a) Landsat ETM⁺ (7, 4, 2) false color mosaic image of Egypt (Geology.com[®] 2008). (b) ASTER (3, 2, 1) true color image of Fawakhir area.

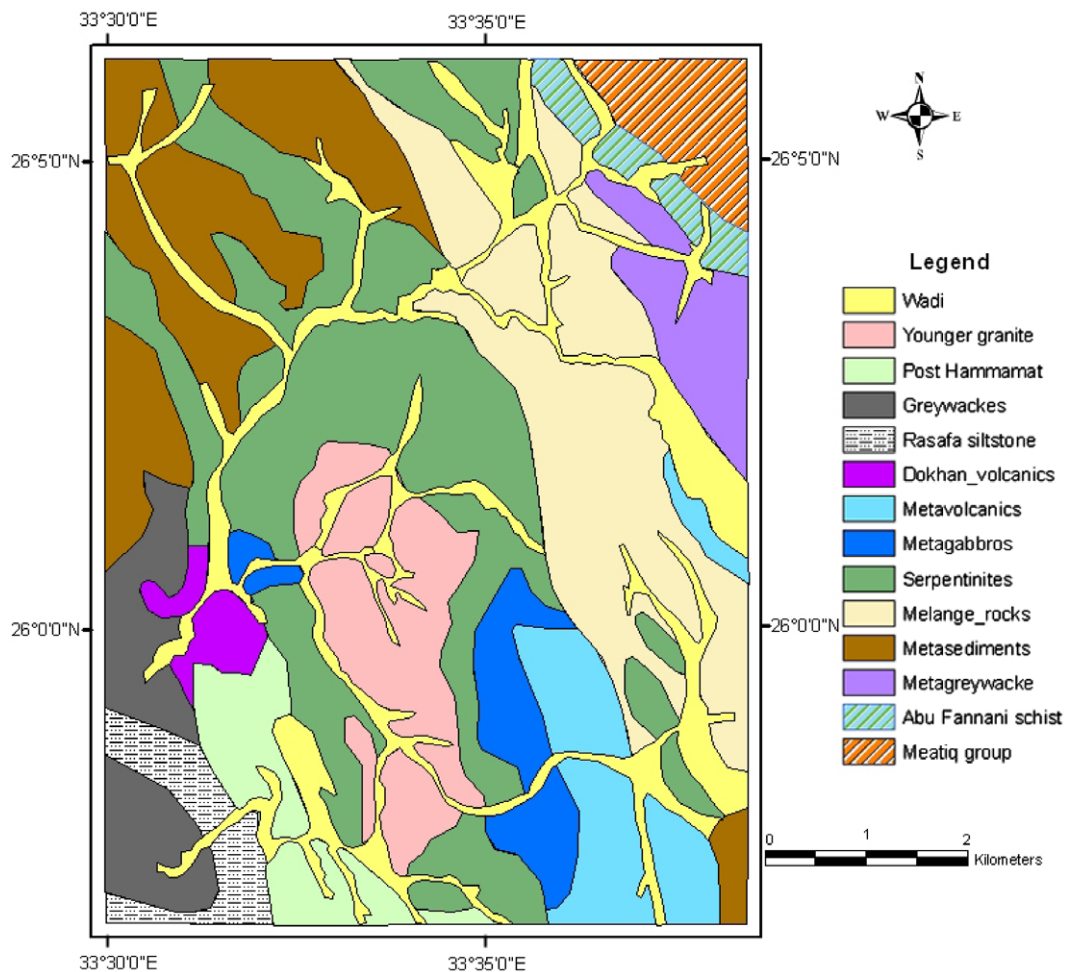


Fig. 2. Lithologic map of Fawakhir area (modified after El-Sayed et al., 1999).

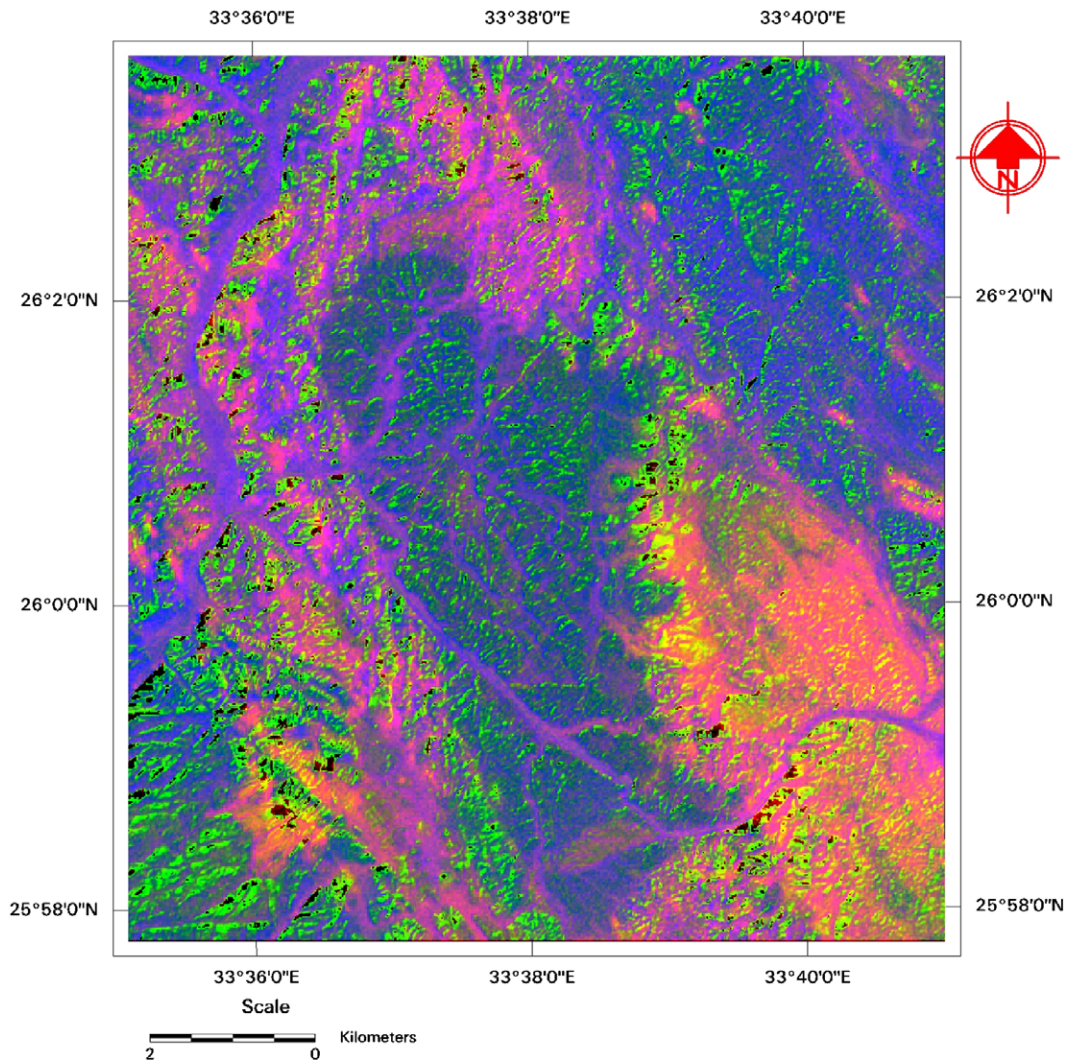


Fig. 3. ASTER band ratio (4/7, 4/1, 2/3 * 4/3) RGB image of (Abdeen et al., 2001).

2. Geologic setting

Ophiolites in the Eastern Desert of Egypt are typically dismembered and form allochthonous bodies of mafic to ultramafic rocks (Ries et al., 1983; Johnson et al., 2004; Stern et al., 2004). A near-complete ophiolitic section has been reported near the Fawakhir gold mine (Garson and Shalaby, 1976; Nasseef et al., 1980). The Fawakhir ophiolite sequence is composed mainly of serpentinites, metagabbros, boninitic metagabbros, and metavolcanics (El-Sayed et al., 1999). The ophiolite is intruded by post-tectonic younger granites and later mafic to acidic dykes that cut all of the Fawakhir ophiolite units (Fig. 2).

The serpentinite rocks surrounding the Fawakhir granitoid pluton are regarded as a member of an ophiolitic sequence developed in a supra-subduction zone setting (El-Mezayen, 1983); There is no thermal metamorphic effect of the serpentinite on the adjacent rocks and the contact between the serpentinite and the underlying mélangé rocks is sharp and marked by a thrust fault striking NNW-SSE (Hassanen, 1985). At Wadi El Sid the serpentinites are intruded by post-tectonic granites and contain large granite apophyses.

The ophiolitic metagabbros in the study area are closely associated with other ophiolitic members' serpentinites and metabasalts. Metagabbros form an elongate body that displays layering on a regional scale, where coarse-grained metagabbros are located at the

base of the mountain and then grade upward to medium-grained rocks at intermediate level and are fine-grained at the top. The metagabbro contact with the serpentinites is highly sheared, mylonitized and foliated with the development of schistose amphibolite rocks (El-Sayed et al., 1999).

The ophiolitic metabasalts are exposed as an elongate body and thrust over the serpentinites. They are intruded by Fawakhir granite which was emplaced after the ophiolitic thrust sheets. The Fawakhir granite pluton is composed of two compositionally distinct granitic phases: an earlier grey monzodiorite phase intruded with sharp contact by a larger pink mainly monzogranite phase (Fowler, 2001). The pluton is inhomogeneous, varying in composition and in color. It is composed of different varieties ranging from granodiorite and hornblende granite along the marginal parts of the pluton, particularly near the El Sid gold mine to differentiated pale pink biotite granite (Harraz and Ashmawy, 1994). These rocks are cut by quartz veins striking nearly NE-SW where El Sid gold mine is located.

3. Data and methods

ASTER has three sensors to measure and record the reflected and emitted Electromagnetic Radiation (EMR). They are working

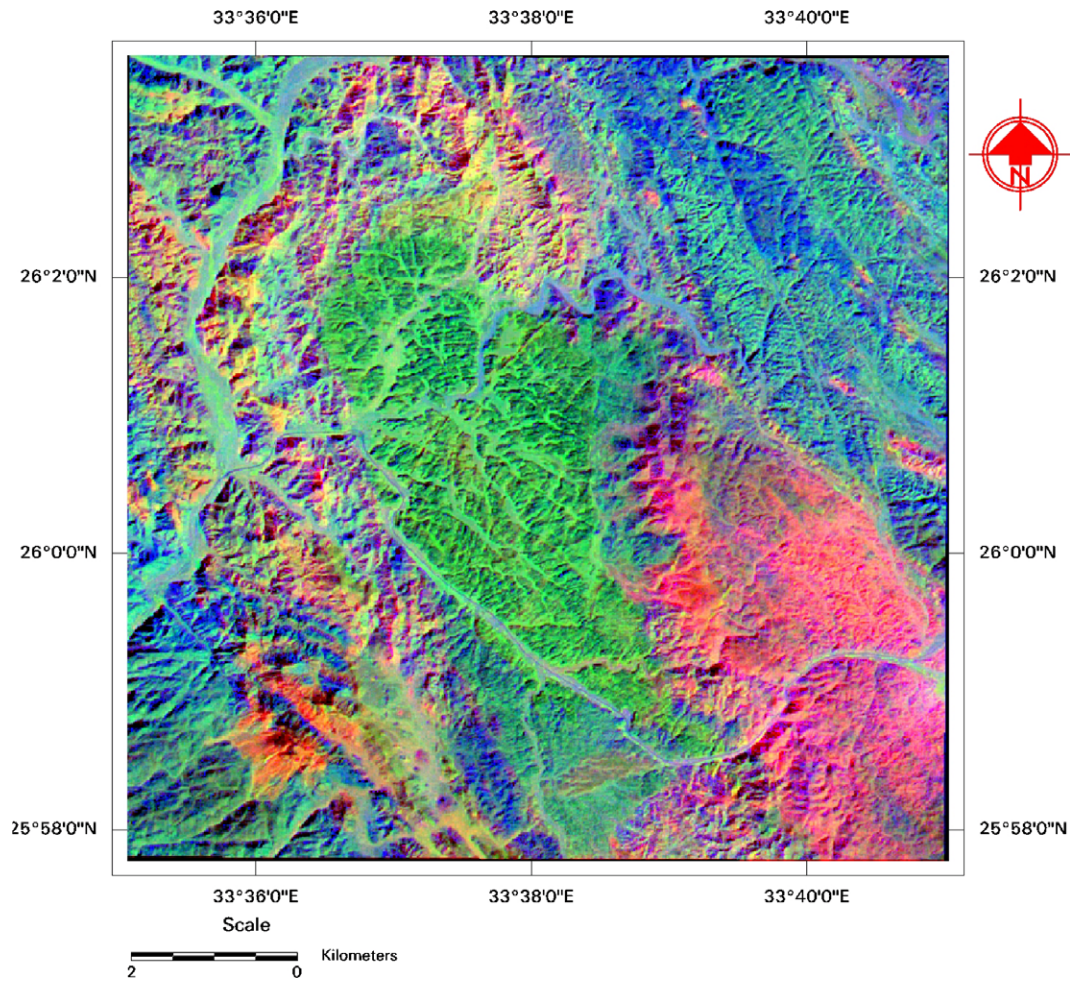


Fig. 4. ASTER band ratio (4/7, 3/4, 2/1) RGB image of (Abdeen et al., 2001).

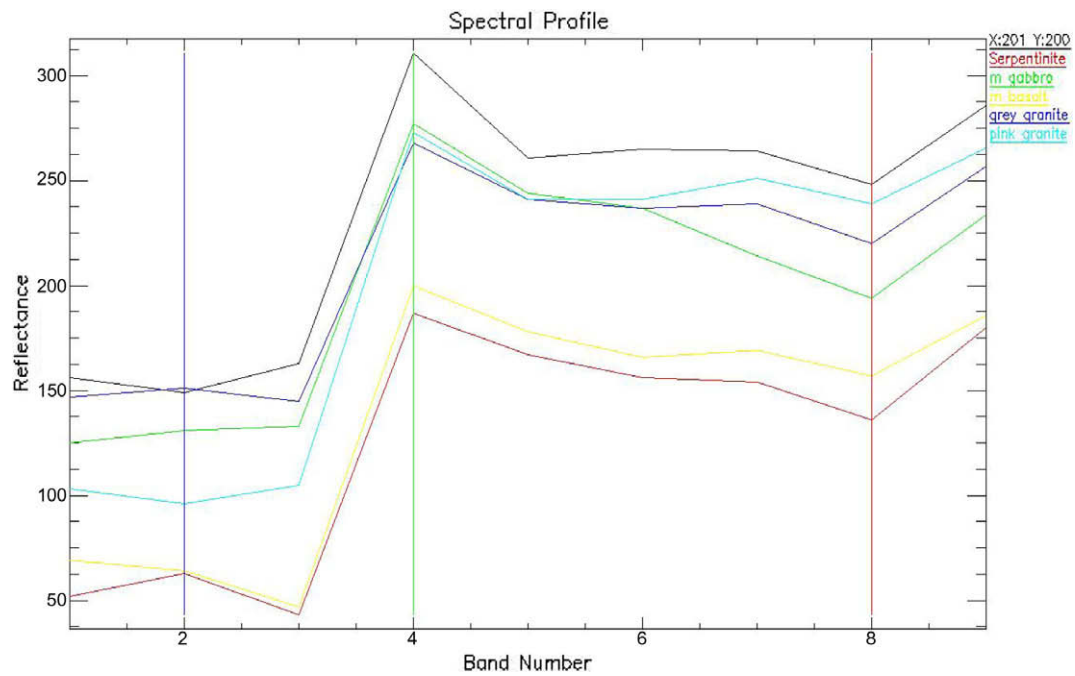


Fig. 5. ASTER image spectra of lithologic units; serpentinites (red), metagabbros (green), metabasalt (yellow), grey granite (blue), and pink granite (cyan). (For interpretation of the references to colour in this figure legend, the reader is referred to the web version of this article.)

in different wavelength regions the Visible and Near Infrared (VNIR) between 0.52 and 0.86 μm, Short Wave Infrared (SWIR) between 1.6 and 2.43 μm, and Thermal Infrared (TIR) between 8.125 and 11.65 μm. ASTER data consists of 14 spectral bands 3 VNIR, 6 SWIR, and 5 TIR with 15, 30, and 90 m spatial resolution, respectively. The VNIR, SWIR and TIR wavelength regions provide complementary data for lithological mapping.

ASTER surface reflectance scene of the study area was processed and analyzed by ENVI (4.5), ERDAS IMAGINE (9.1) and ArcGIS (9.2) software. The ASTER 30-m resolution SWIR data were resampled to correspond to the VNIR 15-m spatial dimensions. Nearest neighbor resampling method uses the nearest pixel values without any interpolation so it was used to maintain the original pixel values of the image. The 15-m resolution 6 SWIR and 3 VNIR bands were combined to form 9-band 15 m spatial resolution data sets.

4. Results

4.1. ASTER band ratios

Band ratioing techniques are used to enhance the spectral differences between bands and reduce the shadow effects caused by topography. Band ratios (4/7, 4/1, 2/3 * 4/3) of ASTER image (Fig. 3), which is equivalent to (5/7, 5/1, 3/4 * 5/4) of Landsat TM (Sultan's combination), and (4/7, 3/4, 2/1) ASTER image (Fig. 4) which is equivalent to (5/7, 4/5, 3/1) Landsat TM image (Abram's combination) are used by (Abdeen et al., 2001) for mapping serpentinite, granite and marble lithologic units of the Neoproterozoic Allaqi Suture in southern Eastern Desert of Egypt.

Image spectral reflectance of lithologic units (serpentinites, metagabbros, metabasalts, grey granite, and pink granite) shows absorption features around bands 3, 6, and 8 (Fig. 5). Image spectra

were used as a reference to construct new ASTER band ratios image where, for each absorption feature, the numerator is the sum of the bands representing the shoulders, and the denominator is the band located nearest the absorption feature minimum. Therefore, we present a better ASTER band ratio ((2 + 4)/3, (5 + 7)/6, (7 + 9)/8) for mapping ophiolites (serpentinites, metagabbros, and metabasalts), granites, and general lithological mapping in arid regions (Fig. 6).

The geologic interpretations of ASTER band ratios ((2 + 4)/3, (5 + 7)/6, (7 + 9)/8) image show that the different lithologic units and the contact between them can be better identified. For validation of the newly developed ASTER band ratio image (Fig. 6) comparison with previously used ASTER band ratios in other areas in the Eastern Desert of Egypt is carried out. The results show that the serpentinites in ASTER band ratios (4/7, 4/1, 2/3 * 4/3) image (Fig. 3) is not distinguished from the metagabbros and Dokhan volcanics and Hammamat sediments, metagabbros can not be separated from the metabasalts, and granites are similar in color to the mélange rocks. In ASTER band ratios (4/7, 3/4, 2/1) image (Fig. 4) serpentinites are not well separated from the adjacent rocks and metagabbros and metabasalts have similar color but granites are separated from adjacent rocks. In our new ASTER band ratios ((2 + 4)/3, (5 + 7)/6, (7 + 9)/8) image (Fig. 6) lithologic units are well differentiated. Serpentinites are well separated from adjacent rocks by light green color, metagabbros have pink color, metabasalts are dark green in color, grey granite has pale violet color and pink granite has a violet color.

4.2. ASTER principal component analysis

Principal Component Analysis (PCA) is used to produce uncorrelated output bands, to segregate noise components, and to reduce

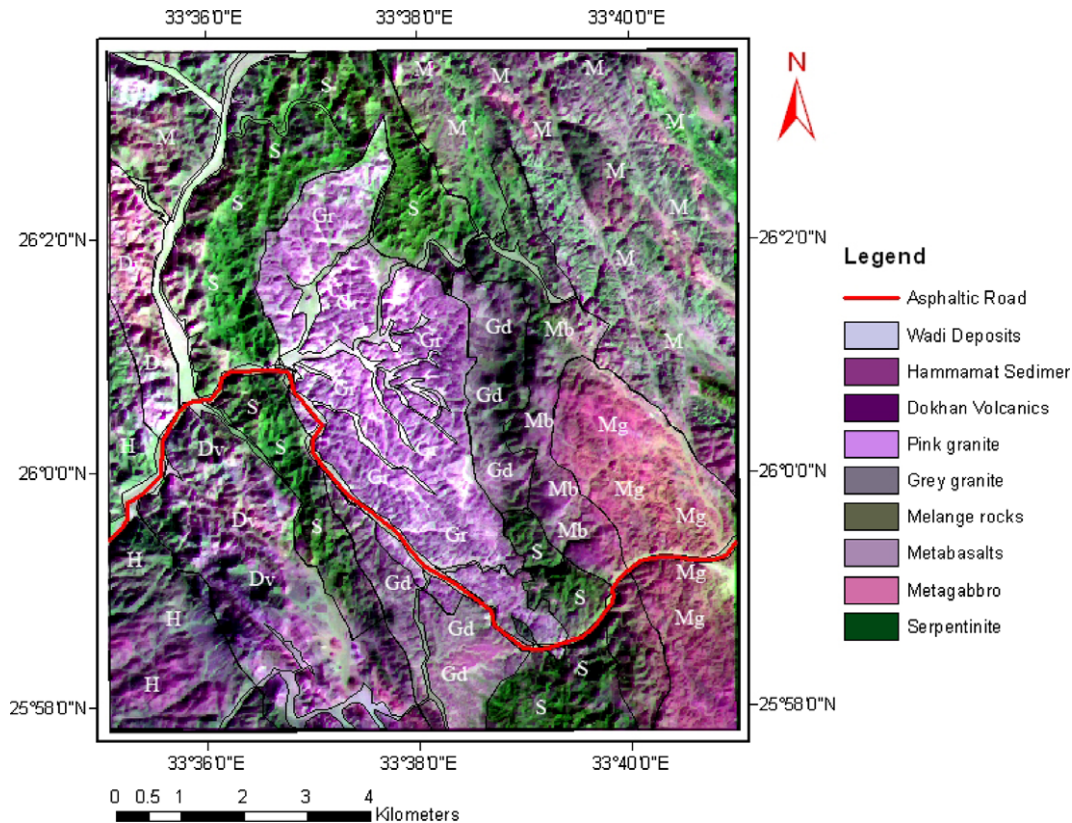


Fig. 6. ASTER band ratio ((2 + 4)/3, (5 + 7)/6, (7 + 9)/8) RGB image; (S) serpentinite, (Mg)metagabbro, (Mb) metabasalt, (M) mélange rocks, (Gd) grey granite, (Gr) pink granite, (Dv) Dokhan volcanics, (H) Hammamat sediments. (For interpretation of the references to colour in this figure legend, the reader is referred to the web version of this article.)

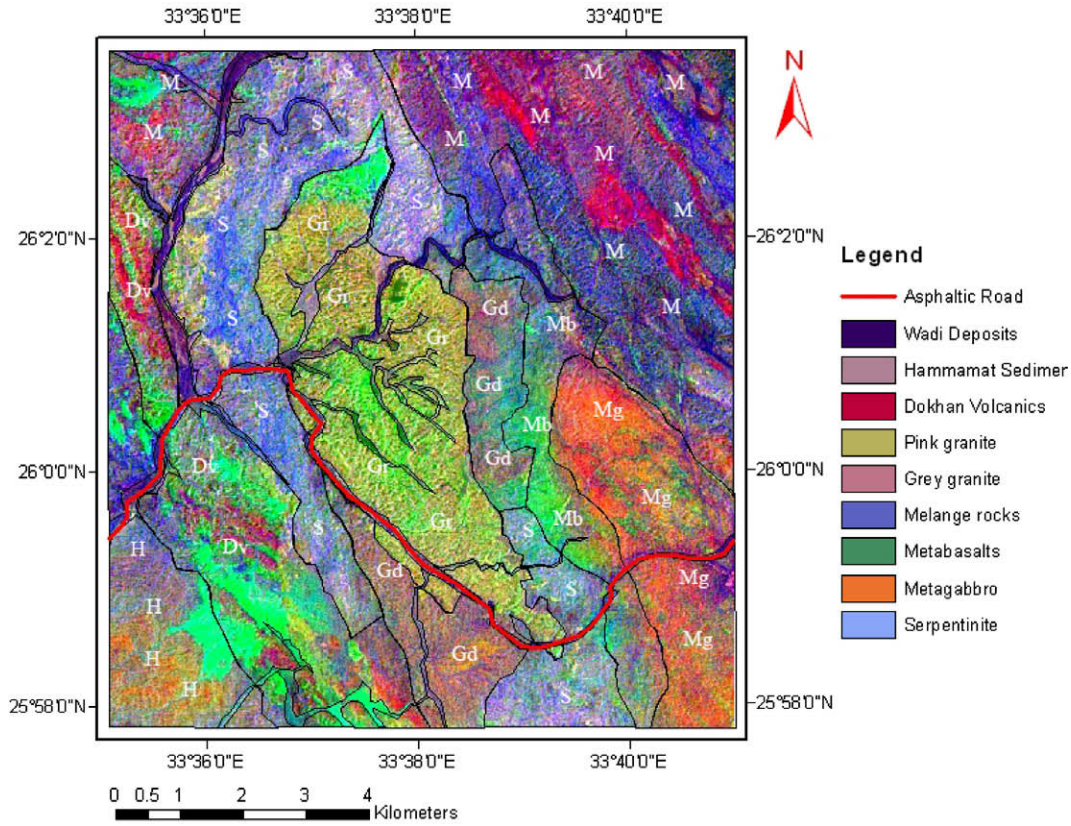


Fig. 7. ASTER Principal Component Analysis (PC5, PC4, and PC2) RGB image; (S) serpentinite, (Mg) metagabbro, (Mb) metabasalt, (M) mélange rocks, (Gd) grey granite, (Gr) pink granite, (Dv) Dokhan volcanics, (H) Hammamat sediments. (For interpretation of the references to colour in this figure legend, the reader is referred to the web version of this article.)

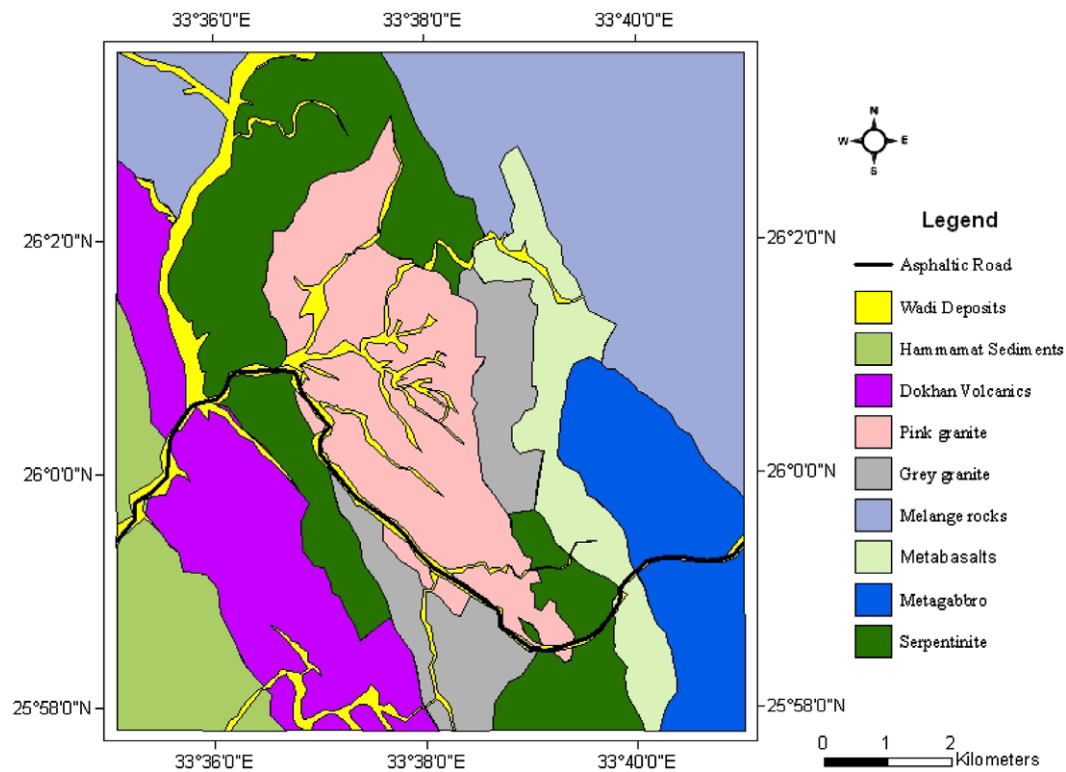


Fig. 8. Lithological map of Fawakhir area.

the dimensionality of data sets. This is done by finding a new set of orthogonal axes that have their origin at the data mean and that are rotated so that the data variance is maximized. It is possible to calculate the same number of output PCA bands as input spectral bands. The first PCA band contains the largest percentage of data variance and the second PCA band contains the second largest data variance, and so on; the last PCA bands appear noisy because they contain very little variance, much of which is due to noise in the original spectral data. Nine bands PCA is constructed from the original 9-band (VNIR & SWIR) ASTER image. From the output PCA 9-bands we selected three bands (PC5, PC4, and PC2) for better discrimination between ophiolitic rocks (serpentinites, metagabbros, and metabasalt), and granite (Fig. 7).

The geologic interpretations of PCA (PC5, PC4, and PC2) image show that serpentinites are identified by pale blue colors, metagabbros have red colors, metabasalts have green colors, grey granite has brown colors and pink granite has a yellowish green color. The PCA image shows better discrimination between grey granite and pink granite more than the band ratios image.

According to previous results, it is evident that the ASTER band ratio image $((2 + 4)/3, (5 + 7)/6, (7 + 9)/8)$ and Principal Component Analysis (PC5, PC4, and PC2) are powerful in distinguishing the subtle differences between the various rock units in the study area. Field observations in the Fawakhir area, aimed at mapping the different rock units and contacts, support the results obtained from the ASTER band ratios and PCA images. The field data are subsequently used together with the results of visual interpretation of the different ASTER images to prepare a detailed lithological map for the Fawakhir area (Fig. 8). This map shows differences in the distribution of some rock units and contacts between them compared to the published geologic map of El-Sayed et al. (1999; Fig. 2). The most prominent differences are the distinguishing between grey and pink granite, metagabbros, and metabasalts, also the contacts between serpentinite and adjacent rocks.

5. Discussion

The image spectral reflectance or the spectra of rock units in the study area serpentinites, metagabbros, metabasalts, grey granite, and pink granite are derived from the ASTER reflectance image (Fig. 5). The shapes of the spectral profiles of the different lithologic units are similar. However, they can be distinguished from one another based on the differences in reflectance relative to different ASTER bands. All lithologic units give higher reflectance in SWIR more than VNIR. Granitic rocks give higher reflectance than the metagabbros, metabasalts, and serpentinites which indicate that mafic rocks absorb more of the electromagnetic radiation and reflect fewer amounts than felsic rocks. All of the rock units show absorption features around bands 3 (0.78–0.86 μm) and 8 (2.295–2.365 μm). Serpentinites and metabasalts show clear absorption features around band 6 (2.185–2.225 μm) whereas metagabbros, grey granite and pink granite show absorption feature between bands 5 (2.145–2.185 μm) and 6 (2.185–2.225 μm).

The USGS spectral library (<http://www.speclab.cr.usgs.gov>) of rock forming minerals was used to evaluate the results of ASTER image spectral signature of the lithologic units in the study area. The results show that serpentine which is the main component of serpentinite has two absorption features at 1.4 and 2.35 μm . Metagabbros and metabasalts consists mainly of pyroxene has absorption feature at 2.35 μm , anorthitic plagioclase has two absorption features around 2 and 2.4 μm , and olivine has absorption features between 0.8 and 1.2 μm . Granite consists of albitic plagioclase and has absorption features around 1.4 and 2.15 μm , orthoclase has absorption features around 2 μm , quartz has absorption features at 2.15 μm , muscovite has absorption features

at 1.4 and 1.15 μm , biotite has absorption features at 2.15 μm . These results almost correspond to the ASTER image derived spectra.

Band ratioing between the high reflectance band and the absorption band of a feature is used to highlight it (i.e. band ratio $4/3$ of high reflectance band 4 and absorption band 3 for vegetation). Band ratio $((2 + 4)/3)$ highlights the serpentinites and metabasalts, $(5 + 7)/6$ highlights the granitic rocks, and $(7 + 9)/8$ highlights the metagabbros and serpentinites. These band ratios were used in red, green and blue to produce a color image to distinguish between the ophiolitic and granitic rocks in Fawakhir area (Fig. 6).

It is generally accepted that the first three high order principal components (1, 2, and 3) have over 99% of spectral information; hence these have been widely used for lithological mapping rather than the subsequent low order principal components (4, 5, 6, etc.) which usually contain less than 1% of spectral information and they contain low signal-to-noise ratios. The higher order principal components provide subtle information about the occurrence of mineral and rock types that are spatially dominant in the image. So, it is interesting to use a combination of certain lower order components which takes up some of the information with higher order principal components to highlight some target spectral signatures. In this study the lowest order PCA 5th component shows some interesting signature in metagabbros, PCA 4 highlights the post-tectonic younger granite and metabasalts, and PCA 2 highlights the serpentinites. So, PCA (PC5, PC4, and PC2) give information to discriminate old granite from younger granite and metabasalts from metagabbros much better than (PC1, PC2, and PC3). Overall, PCA is statistics-based and results may differ in the same area with different geographic sizes.

6. Conclusions

The newly developed ASTER band ratios and Principal Component Analysis PCA images are used to distinguish between ophiolitic rocks which include (serpentinite, metagabbro, and metabasalt) and granitic rocks (grey and pink granites) of the Fawakhir area. It is recommended using ASTER band ratios $((2 + 4)/3, (5 + 7)/6, (7 + 9)/8)$ in RGB for mapping serpentinites and Principal Component Analysis (PC5, PC4, and PC2) in RGB to discriminate between the different types of granitic rocks and ophiolitic rocks. Comparison between the results derived from the proposed new methods and field work demonstrate that the new methods were successful in lithological mapping of Fawakhir area. Therefore, we suggest that these techniques may be used as time- and cost-effective approach for lithological mapping in the Arabian Nubian shield and other arid areas.

References

- Abdeen, M.M., Allison, T.K., Abdelsalam, M.G., Stern, R.J., 2001. Application of ASTER band-ratio images for geological mapping in arid regions; the Neoproterozoic Allaqi Suture, Egypt. Abstract with Program Geological Society of America 3 (3), 289.
- Abrams, M.J., Brown, D., Lepley, L., Sadowski, R., 1983. Remote sensing for porphyry copper deposits in southern Arizona. *Economic Geology* 78, 591–604.
- Abrams, M.J., Hook, S.J., 1995. Simulated ASTER data for geologic studies. *IEEE Transactions of Geoscience and Remote Sensing* 33, 692–699.
- El-Mezayen, A.M.A., 1983. Geology and petrology of the basement rocks in the Fawakhir area, Central Eastern Desert, Egypt 'El Fawakhir ophiolites'. Ph.D. Thesis, Al-Azhar University, Egypt, 248p.
- El Ramly, M.F., Greiling, R.O., Rashwan, A.A., Ramsy, A.H., 1993. Explanatory note to accompany the geological and structural maps of Wadi Hafafit area, Eastern Desert of Egypt. *Annual Geological Survey Egypt* 9, 1–53.
- El-Sayed, M.M., Furnes, H., Mohamed, F.H., 1999. Geochemical constraints on the tectonomagmatic evolution of the late Precambrian Fawakhir ophiolite, Central Eastern Desert, Egypt. *Journal of African Earth Sciences* 29, 515–533.
- Fowler, T.J., 2001. Pan-African granite emplacement mechanisms in the Eastern Desert, Egypt. *Journal of African Earth Sciences* 32 (1), 61–66.

- Gad, S., Kusky, T.M., 2006. Lithological mapping in the Eastern Desert of Egypt, the Barramiya area, using Landsat thematic mapper (TM). *Journal of African Earth Sciences* 44, 196–202.
- Gad, S., Kusky, T.M., 2007. ASTER spectral ratioing for lithological mapping in the Arabian-Nubian shield, the Neoproterozoic Wadi Kid area, Sinai, Egypt. *Gondwana Research* 11 (3), 326–335.
- Garson, M.S., Shalaby, I., 1976. Precambrian-lower Palaeozoic plate tectonics and metallogenesis in the Red Sea region. *Geologic Association Canada, Special Paper* 14, pp. 573–596.
- Harraz, H.Z., Ashmawy, M.H., 1994. Structural and lithochemica constraints on the localization of gold deposits at the El Sid-Fawakhir Gold Mine area, Eastern Desert, Egypt. *Egyptian Journal Geology* 38, 629–648.
- Hassanen, M.A., 1985. Petrology and geochemistry of ultramafic rocks in the Eastern Desert, Egypt, with special reference to Fawakhir area. Ph.D. Dissertation, Alexandria University, Egypt, 348p.
- Johnson, P.R., Kattan, F.H., Al-Saleh, A.M., 2004. Neoproterozoic ophiolites in the Arabian Shield: Field relations and structure. In: Kusky, T.M. (Ed.), *Precambrian Ophiolites and Related Rocks, Developments in Precambrian Geology*, vol. 13. Elsevier, Amsterdam, pp. 129–162.
- Kusky, T.M., Abdelsalam, M.G., Tucker, R.D., Stern, R.J., 2003. Evolution of the East African and related orogens, and the assembly of Gondwana. *Precambrian Research* 123 (2–4), 81–337.
- Mars, J.C., Rowan, L.C., 2006. Regional mapping of phyllic- and argillic-altered rocks in the Zagros magmatic arc, Iran, using Advanced Spaceborne Thermal Emission and Reflection Radiometer (ASTER) data and logical operator algorithms. *Geosphere* 2 (3), 161–186.
- Nasseef, A.O., Bakor, A.R., Hashad, A.H., 1980. Petrography of possible ophiolitic rocks along Qift-Quseir road, Eastern Desert, Egypt. *Inst. Appl. Geol. Jeddah, Bull.* 3 (4), 77–82.
- Ries, A.C., Shackleton, R.M., Graham, R.h., Fitches, W.R., 1983. Pan-African structures, ophiolites and mélangé in the Eastern Desert of Egypt: a traverse at 26°N. *Journal of the Geological Society* 140 (1), 75–95.
- Rowan, L.C., Mars, J.C., 2003. Lithologic mapping in the Mountain Pass, California area using Advanced Spaceborne Thermal Emission and Reflection Radiometer (ASTER) data. *Remote Sensing of Environment* 84 (3), 350–366.
- Rowan, L.C., Hook, S.J., Abrams, M.J., Mars, J.C., 2003. Mapping hydrothermally altered rocks at Cuprite, Nevada, using the Advanced Spaceborne Thermal Emission and Reflection Radiometer (ASTER). A new satellite-imaging system. *Economic Geology* 98 (5), 1019–1027.
- Sabins, F., 1997. *Remote Sensing Principles and Interpretation*, third ed., 494pp.
- Stern, R.J., 1994. Arc assembly and continental collision in the Neoproterozoic East African orogen implications for consolidation of Gondwanaland. *Annual Review of Earth and Planetary Sciences* 22, 319–351.
- Stern, R.J., Johnson, P., Kröner, A., Yibas, B., 2004. Neoproterozoic Ophiolites of the Arabian-Nubian Shield. In: Kusky, T.M. (Ed.), *Precambrian Ophiolites and Related Rocks*. In: *Developments in Precambrian Geology*, vol. 13. Elsevier, Amsterdam, pp. 95–128.
- Sultan, M., Arvidson, R.E., Sturchio, N.C., 1986. Mapping of serpentinites in the Eastern Desert of Egypt by using Landast Thematic Mapper data. *Geology* 14, 995–999.
- USGS Mineral Spectral Library. <<http://www.speclab.cr.usgs.gov>>.